

# Long-range magnetic ordering of $S = 1/2$ linear trimers in $A_3\text{Cu}_3(\text{PO}_4)_4$ ( $A = \text{Ca}, \text{Sr}, \text{and Pb}$ )

Alexei A. Belik<sup>a,b,\*</sup>, Akira Matsuo<sup>c</sup>, Masaki Azuma<sup>a,b</sup>, Koichi Kindo<sup>c</sup>, Mikio Takano<sup>a</sup>

<sup>a</sup>Institute for Chemical Research, Kyoto University, Uji, Kyoto-fu 611-0011, Japan

<sup>b</sup>PRESTO, Japan Science and Technology Corporation (JST), Kawaguchi, Saitama 332-0012, Japan

<sup>c</sup>KYOKUKEN, Osaka University, Toyonaka, Osaka 560-8531, Japan

Received 30 September 2004; received in revised form 10 December 2004; accepted 15 December 2004

## Abstract

Magnetic properties of  $S = 1/2$  linear trimer cluster compounds  $A_3\text{Cu}_3(\text{PO}_4)_4$  ( $A = \text{Ca}, \text{Sr}, \text{and Pb}$ ) were investigated. Magnetic susceptibility data for the three compounds showed that paramagnetic copper spins form trimers with the total spin of  $1/2$  below about 45 K. Specific heat and magnetization measurements indicated that the trimer clusters undergo ferromagnetic long-range ordering at  $T_C = 0.91$  K for  $A = \text{Ca}$  and antiferromagnetic long-range ordering at  $T_N = 0.91$  K for  $A = \text{Sr}$  and  $T_N = 1.26$  K for  $A = \text{Pb}$ .  $A_3\text{Cu}_3(\text{PO}_4)_4$  exhibited  $1/3$ -magnetization plateau at least up to magnetic field of 55 T at 1.3 and 4.2 K.  $A_3\text{Cu}_3(\text{PO}_4)_4$  with  $A = \text{Sr}$  and  $\text{Pb}$  showed a spin-flop transition near 0.03 T in the antiferromagnetic state at 0.08 K. Specific heat data at magnetic fields clearly showed broad maxima at low temperatures due to the finite intra-chain interaction in one-dimensional arrays of the trimers. © 2005 Elsevier Inc. All rights reserved.

**Keywords:** Heisenberg antiferromagnet; Trimer system; Magnetic susceptibility; Specific heat; High-field magnetization

## 1. Introduction

Low-dimensional quantum magnets have been a subject of intense studies in recent years. In particular, zero-dimensional (cluster) systems with spin ( $S$ ) of  $1/2$  is considered to be interesting because the quantum effects are much pronounced.

Magnetic interactions ( $J_1$  and  $J_2$ ) between copper atoms in two isostructural compounds  $A_3\text{Cu}_3(\text{PO}_4)_4$  ( $A = \text{Ca}$  [1] and  $\text{Sr}$  [2]), belonging to space group  $P2_1/c$ , are shown on Fig. 1a. They can be presented by the one-dimensional (1D) array of trimer clusters, where the trimers possessing the total spin of  $1/2$  are connected on one direction. In other words, it is a kind of 1D ferrimagnet. There are two copper sites. The Cu1 site

has a square planar coordination and the Cu2 site has a distorted square pyramidal coordination. Cu1 and Cu2 are connected with each other through a common oxygen atom. By analyzing the magnetic susceptibility and specific heat ( $T = 1.8$ – $15$  K) data [3–5], the intra-trimer exchange constant ( $J_1$ ) was estimated to be about 100 K, while the inter-trimer exchange constant ( $J_2$ ) about 3 K. Thus,  $J_1$  is much larger than  $J_2$  and  $A_3\text{Cu}_3(\text{PO}_4)_4$  is a model system of the  $S = 1/2$  linear Heisenberg antiferromagnetic trimer [6].  $\text{Ca}_3\text{Cu}_3(\text{PO}_4)_4$  was reported to order ferromagnetically at 0.8 K, while  $\text{Sr}_3\text{Cu}_3(\text{PO}_4)_4$  exhibits an antiferromagnetic ordering at 0.9 K [4]. Thus, the inter-chain (Fig. 1b) interactions are also expected to be very small. Magnetization measurements up to 40 T showed the existence of  $1/3$ -magnetization plateau [7]. In addition, magnetic susceptibility curves of  $A_3\text{Cu}_3(\text{PO}_4)_4$  ( $A = \text{Ca}$  and  $\text{Sr}$ ) exhibit a clear signature of 1D ferrimagnets, i.e., a rounded minimum of  $\chi T$  near 25 K and strong increase of  $\chi T$  at the lower temperatures [3,4].

\*Corresponding author. International Center for Young Scientists, National Institute for Materials Science, Namiki 1-1, Tsukuba, Ibaraki, 305-0044, Japan. Fax: +81 29 860 4706.

E-mail address: [alexei.belik@nims.go.jp](mailto:alexei.belik@nims.go.jp) (A.A. Belik).

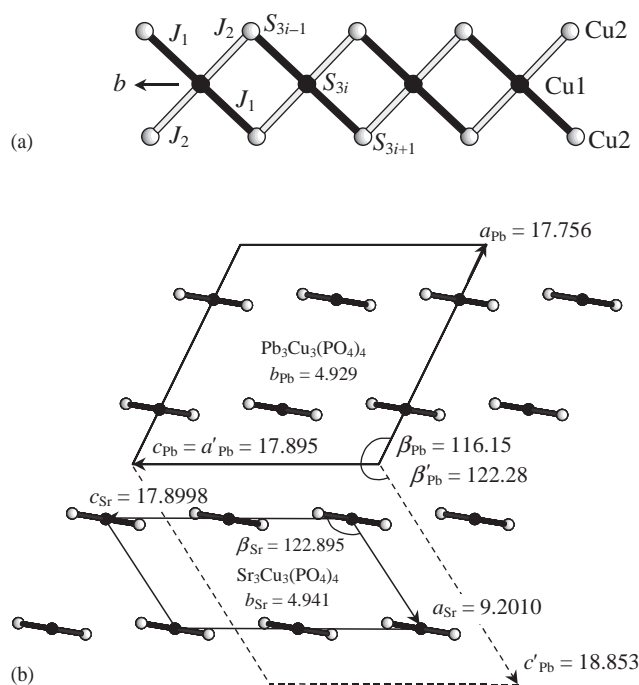


Fig. 1. (a) Projection of the 1D copper trimeric chain on the  $bc$  plane in  $\text{Sr}_3\text{Cu}_3(\text{PO}_4)_4$  and  $\text{Pb}_3\text{Cu}_3(\text{PO}_4)_4$ . The intra-trimer ( $J_1$ : black stick) and intra-chain ( $J_2$ : white stick) interactions are shown. (b) Projection of the structures of  $\text{Sr}_3\text{Cu}_3(\text{PO}_4)_4$  and  $\text{Pb}_3\text{Cu}_3(\text{PO}_4)_4$  along the  $b$  axes: arrangement of the 1D copper chains. Unit cells for  $\text{Sr}_3\text{Cu}_3(\text{PO}_4)_4$  and  $\text{Pb}_3\text{Cu}_3(\text{PO}_4)_4$  are shown by solid lines and lattice parameters ( $a$ ,  $b$ , and  $c$  in Å and  $\beta$  in deg) are given. For  $\text{Pb}_3\text{Cu}_3(\text{PO}_4)_4$ , the monoclinic cell ( $a'$ ,  $c'$ , and  $\beta'$ ) in another setting ( $I2/a$ ) is shown by the broken line.

Recently, a new compound  $\text{Pb}_3\text{Cu}_3(\text{PO}_4)_4$ , crystallizing in space group  $C2/c$ , was reported [8]. The lattice parameters of  $\text{Sr}_3\text{Cu}_3(\text{PO}_4)_4$  ( $a_{\text{Sr}}$ ,  $b_{\text{Sr}}$ ,  $c_{\text{Sr}}$ , and  $\beta_{\text{Sr}}$ ) have the following relation with those of  $\text{Pb}_3\text{Cu}_3(\text{PO}_4)_4$  ( $a'_{\text{Pb}}$ ,  $b'_{\text{Pb}}$ ,  $c'_{\text{Pb}}$ , and  $\beta'_{\text{Pb}}$ ):  $a_{\text{Sr}} \approx 0.5c'_{\text{Pb}}$ ,  $b_{\text{Sr}} \approx b'_{\text{Pb}}$ ,  $c_{\text{Sr}} \approx a'_{\text{Pb}}$ , and  $\beta_{\text{Sr}} \approx \beta'_{\text{Pb}}$  (Fig. 1b). The coordination polyhedra of Cu and Sr(Pb) atoms are the same in  $\text{Sr}_3\text{Cu}_3(\text{PO}_4)_4$  and  $\text{Pb}_3\text{Cu}_3(\text{PO}_4)_4$ , that is,  $\text{Cu}1\text{O}_4$ ,  $\text{Cu}2\text{O}_5$ ,  $\text{Sr}1(\text{Pb}1)\text{O}_6$ , and  $\text{Sr}2(\text{Pb}2)\text{O}_9$ .  $\text{Pb}_3\text{Cu}_3(\text{PO}_4)_4$  has the similar 1D chains of the copper trimers as shown on Fig. 1a. However, the arrangement of the 1D chains is different in  $\text{Sr}_3\text{Cu}_3(\text{PO}_4)_4$  and  $\text{Pb}_3\text{Cu}_3(\text{PO}_4)_4$ . While the projection of the 1D chains along the  $b$  axes is the same in  $\text{Sr}_3\text{Cu}_3(\text{PO}_4)_4$  and  $\text{Pb}_3\text{Cu}_3(\text{PO}_4)_4$  (Fig. 1b), the adjacent 1D chains have different orientations as can be seen on the projection along the  $a_{\text{Sr}}$  axis in  $\text{Sr}_3\text{Cu}_3(\text{PO}_4)_4$  and along the  $(a_{\text{Pb}} + c_{\text{Pb}})$  vector in  $\text{Pb}_3\text{Cu}_3(\text{PO}_4)_4$  (Fig. 2). Note that  $\text{Ca}_3\text{Cu}_3(\text{PO}_4)_4$  and  $\text{Sr}_3\text{Cu}_3(\text{PO}_4)_4$  prepared by the solid state method are isotypic with each other [2].  $\text{Sr}_3\text{Cu}_3(\text{PO}_4)_4$  prepared by hydrothermal methods is topologically similar but not isotypic with  $\text{Ca}_3\text{Cu}_3(\text{PO}_4)_4$  [8]. Magnetic properties of  $\text{Pb}_3\text{Cu}_3(\text{PO}_4)_4$  have not been investigated yet.

In this work, we report on the properties of  $\text{Pb}_3\text{Cu}_3(\text{PO}_4)_4$  studied by magnetic susceptibility, spe-

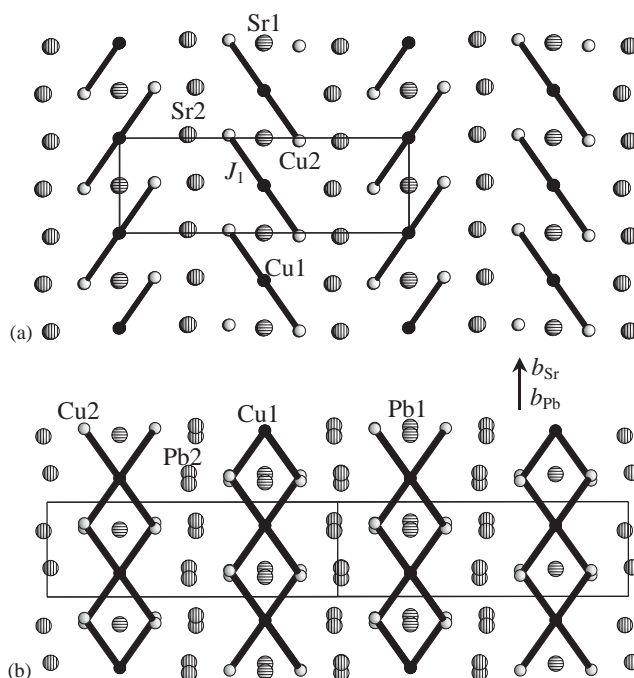


Fig. 2. Projection of the 1D copper trimeric chains in (a)  $\text{Sr}_3\text{Cu}_3(\text{PO}_4)_4$  with the  $a_{\text{Sr}}$  axis perpendicular to this figure and (b)  $\text{Pb}_3\text{Cu}_3(\text{PO}_4)_4$  with the  $(a_{\text{Pb}} + c_{\text{Pb}})$  vector perpendicular to this figure. Sr and Pb atoms are also shown.

cific heat, and magnetization measurements. We also measured magnetization curves up to 55 T and specific heat data in a wider temperature range and in magnetic fields for the related compounds  $A_3\text{Cu}_3(\text{PO}_4)_4$  ( $A = \text{Ca}$  and Sr).

## 2. Experiment section

The samples  $A_3\text{Cu}_3(\text{PO}_4)_4$  ( $A = \text{Ca}$ , Sr, and Pb) were prepared from stoichiometric mixtures of  $\text{CuO}$ ,  $\text{NH}_4\text{H}_2\text{PO}_4$ ,  $\text{CaCO}_3$ ,  $\text{SrCO}_3$ , and  $\text{PbO}$  by the solid state method. The corresponding mixtures were heated very slowly in air from room temperature to 770 K (kept for 20 h), reground, pressed into pellets at 200 kgf/cm<sup>2</sup>, and allowed to react at 1183 K for  $A = \text{Ca}$  and Sr and at 993 K for  $A = \text{Pb}$  on Pt plates for 100 h with four intermediate grindings. X-ray powder diffraction (XRD) data collected with a RIGAKU RINT 2500 diffractometer ( $2\theta$  range of 8–60°, a step width of 0.02°, and a counting time of 1 s/step) showed that the samples were monophasic. Note that the differential thermal analysis (DTA) data showed that  $A_3\text{Cu}_3(\text{PO}_4)_4$  ( $A = \text{Ca}$ , Sr, and Pb) melts incongruently at 1333, 1281, and 1036 K, respectively. The DTA curves also indicated the existence of a reversible phase transition in  $A_3\text{Cu}_3(\text{PO}_4)_4$  ( $A = \text{Ca}$  and Sr) just below (about 10 K) the decomposition temperatures, i.e., at 1324 and 1273 K for  $A = \text{Ca}$  and Sr, respectively.

Magnetic susceptibility ( $\chi = M/H$ ) measurements were performed on a Quantum Design SQUID magnetometer (MPMS XL) between 2 and 400 K in applied fields of 1000 Oe for  $A = \text{Ca}$  and  $\text{Sr}$  and 100 Oe for  $A = \text{Pb}$  under both zero-field-cooled (ZFC) and field-cooled (FC: measured in a magnetic field from 400 to 2 K) conditions. High-field magnetization data were taken at 1.3 and 4.2 K in a pulsed magnetic field up to 55 T and at 0.08 K up to 25 T by an induction method using a multilayer pulse magnet at KYOKUGEN, Osaka University. Specific heat,  $C_p(T)$ , of  $\text{Pb}_3\text{Cu}_3(\text{PO}_4)_4$  was recorded between 0.45 and 300 K (on cooling) at zero magnetic field and between 1.8 and 100 K at magnetic fields of 1, 3, and 5 T by a pulse relaxation method using a commercial calorimeter (Quantum Design PPMS). For  $A_3\text{Cu}_3(\text{PO}_4)_4$  ( $A = \text{Ca}$  and  $\text{Sr}$ ), the  $C_p(T)$  data were taken between 0.45 and 170 K at zero magnetic field and between 1.8 and 50 K at magnetic fields of 1, 3, and 5 T.

### 3. Results and discussion

The temperature dependence of the inverse magnetic susceptibility,  $\chi^{-1}$ , and  $\chi T$  for  $\text{Pb}_3\text{Cu}_3(\text{PO}_4)_4$  is displayed in Fig. 3. No noticeable difference is found between the ZFC and FC curves. The  $\chi^{-1}$  vs.  $T$  curve exhibits a curvature near 45 K. Between 150 and 400 K, the  $\chi^{-1}$  vs.  $T$  curve is fitted by the modified Curie–Weiss equation

$$\chi(T) = \chi_0 + \frac{C}{T - \theta} \quad (1)$$

with the temperature independent term,  $\chi_0$ , of  $-2.53(3) \times 10^{-4} \text{ cm}^3 \text{ K/Cu mol}$ , the Curie constant,  $C$ , of  $0.496(2) \text{ cm}^3 \text{ K/Cu mol}$ , and the Weiss constant,  $\theta$ , of  $-57.0(7) \text{ K}$ . These values show that each Cu ion has spin  $-1/2$  with  $g$  value of 2.30 and these interact antiferromagnetically with each other. Between 7 and 30 K, the fitting to Eq. (1) gave  $\chi_0 = 1.0(4) \times 10^{-4} \text{ cm}^3 \text{ K/Cu mol}$ ,  $C = 0.1585(12) \text{ cm}^3 \text{ K/Cu mol}$ , and  $\theta = 2.77(5) \text{ K}$ . The ratio between the Curie constants at the

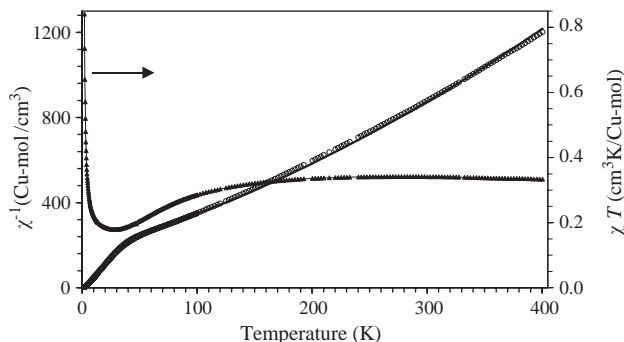


Fig. 3. Inverse magnetic susceptibilities,  $\chi^{-1}$ , and the product  $\chi T$  against temperature,  $T$ , for  $\text{Pb}_3\text{Cu}_3(\text{PO}_4)_4$ . The solid line for the  $\chi^{-1}(T)$  curve is the fit to Eq. (2).

high and low temperature regions,  $C_{\text{HT}}/C_{\text{LT}}$ , is 3.13. The small Curie constant below 45 K indicates that paramagnetic copper spins form trimer clusters because of relatively strong intra-trimer antiferromagnetic interactions and each trimer has a total spin ( $S_{\text{total}}$ ) of  $1/2$ . The  $\chi T$  vs.  $T$  curve of  $\text{Pb}_3\text{Cu}_3(\text{PO}_4)_4$  is similar to those of  $A_3\text{Cu}_3(\text{PO}_4)_4$  ( $A = \text{Ca}$  and  $\text{Sr}$ ) [3,4] and demonstrates the typical features of 1D ferrimagnets, i.e., a rounded minimum near 28 K and then a strong increase at the lower temperatures (Fig. 3).

At the whole temperature range of 2–400 K, the  $\chi^{-1}$  vs.  $T$  curve is fitted by the model of the isolated  $S = 1/2$  Heisenberg linear trimers [5]

$$\chi(T) = \chi_0 + \frac{Ng^2\mu_B^2}{12k_B T} \frac{1 + \exp(J_1/k_B T) + 10 \exp(-J_1/2k_B T)}{1 + \exp(J_1/k_B T) + 2 \exp(-J_1/2k_B T)}, \quad (2)$$

where  $N$  is the Avogadro's number,  $g$  the spectroscopic splitting factor ( $g$ -factor),  $\mu_B$  the Bohr magneton,  $k_B$  the Boltzmann's constant, and  $J_1$  the intra-trimer exchange constant (Fig. 1a) with the Hamiltonian formulated as  $H = J_1 (S_{3i}S_{3i+1} + S_{3i}S_{3i-1})$ . The fitted parameters are  $\chi_0 = -2.97(12) \times 10^{-4} \text{ cm}^3 \text{ K/Cu mol}$ ,  $g = 2.291(13)$ , and  $J_1/k_B = 106(2) \text{ K}$  for  $\text{Pb}_3\text{Cu}_3(\text{PO}_4)_4$ . The  $J_1/k_B$  value determined from the magnetic susceptibility data is close to that found from inelastic neutron scattering experiments ( $J_1/k_B = 106 \text{ K}$ ) [6].

The fitting of our magnetic susceptibility data ( $\chi^{-1}$  vs.  $T$ ) for  $A_3\text{Cu}_3(\text{PO}_4)_4$  ( $A = \text{Ca}$  and  $\text{Sr}$ ) by Eq. (2) yields  $g = 2.32(2)$  and  $J_1/k_B = 127(3) \text{ K}$  for  $A = \text{Ca}$  and  $g = 2.27(2)$  and  $J_1/k_B = 126(3) \text{ K}$  for  $A = \text{Sr}$ . The  $g$  values are in excellent agreement with those determined from the ESR measurements ( $g = 2.3$ ) [7]. However, the  $J_1/k_B$  values are slightly larger than those obtained from inelastic neutron scattering experiments (110 K for  $A = \text{Ca}$  and 117 K for  $A = \text{Sr}$ ) [6].

Specific heat data between 0.45 and 15 K for  $\text{Pb}_3\text{Cu}_3(\text{PO}_4)_4$  are given in Fig. 4. The  $\lambda$ -type peak is

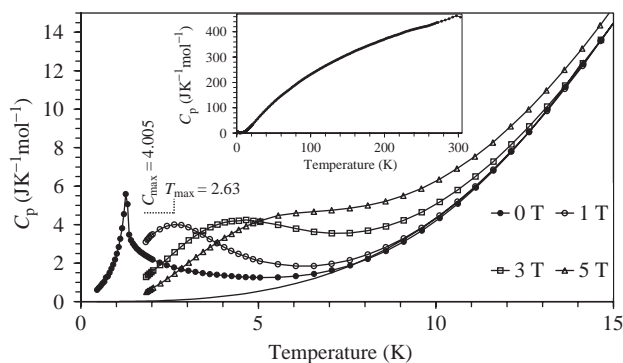


Fig. 4. The  $C_p$  vs.  $T$  curves for  $\text{Pb}_3\text{Cu}_3(\text{PO}_4)_4$  at 0, 1, 3, and 5 T. The parameters of the broad maximum ( $T_{\text{max}}$  (K) and  $C_{\text{max}}$  ( $\text{JK}^{-1} \text{ mol}^{-1}$ )) at 1 T are given. Solid line is the estimated lattice contribution. Inset gives the  $C_p$  vs.  $T$  curve between 0.45 and 300 K.

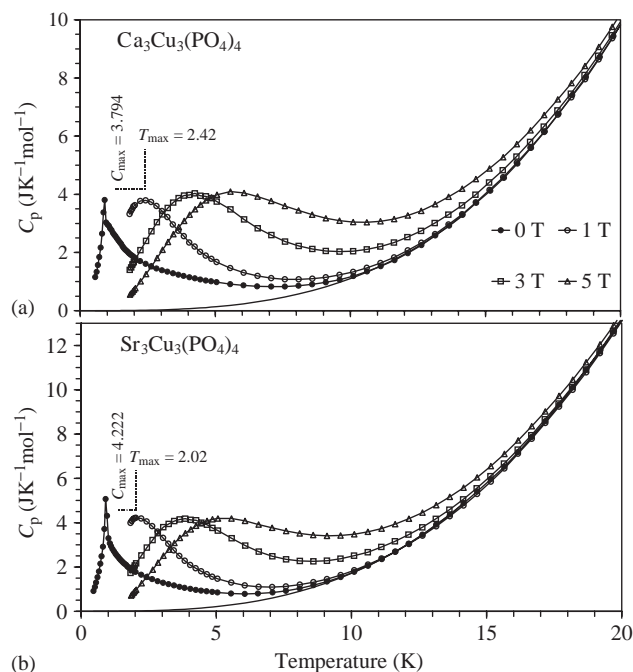


Fig. 5. The  $C_p$  vs.  $T$  curves for (a)  $\text{Ca}_3\text{Cu}_3(\text{PO}_4)_4$  and (b)  $\text{Sr}_3\text{Cu}_3(\text{PO}_4)_4$  at 0, 1, 3, and 5 T. The parameters of the broad maximum ( $T_{\text{max}}$  and  $C_{\text{max}}$ ) at 1 T are given. Solid line is the estimated lattice contribution.

seen at 1.26(3) K indicating long-range magnetic ordering in  $\text{Pb}_3\text{Cu}_3(\text{PO}_4)_4$ . In  $A_3\text{Cu}_3(\text{PO}_4)_4$  ( $A = \text{Ca}$  and  $\text{Sr}$ ), the  $\lambda$ -type peak is observed at 0.91(3) K for both compounds (Fig. 5). This temperature is close to the temperatures of long-range ordering reported in the literature [4]. However, the peaks are rather unusual. For example, the  $C_p$  values for  $\text{Ca}_3\text{Cu}_3(\text{PO}_4)_4$  start to increase gradually at about 7 K with decreasing the temperature and then a sharp peak indicating the long-range ordering appears at 0.91 K. It seems that the peak has two components. It was predicted that the specific heat of the magnetic system given on Fig. 1a has intrinsic double-peak structure [3,9]. One is the Schottky-type peak corresponding to the intra-trimer interaction at about  $0.4J_1$ . The temperature position and the value of the second anomaly depend on the ratio  $J_2/J_1$ . When  $J_2/J_1$  is small enough, the clear second anomaly should be observed at low temperatures on magnetic specific heat,  $C_m$ . In the present data for  $A_3\text{Cu}_3(\text{PO}_4)_4$  ( $A = \text{Ca}$ ,  $\text{Sr}$ , and  $\text{Pb}$ ) taken in zero magnetic field, the second anomalies overlap with the  $\lambda$ -type peaks (Figs. 4 and 5). These anomalies are more pronounced in the data taken in the magnetic fields.

Unfortunately, the numerical calculations of  $C_m$  for the system given in Fig. 1a were done only for antiferromagnetic  $J_2$ , at zero magnetic field, and for  $J_2/J_1 \geq 0.1$  [3,9]. However, the intra-chain interaction in the 1D array of the trimers ( $J_2$ ) may be ferromagnetic as indicated by the positive Weiss constant at the low temperature region. The numerical calculation are

desirable in magnetic fields and for  $|J_2|/J_1 < 0.1$  because they will help to estimate  $J_2$  from the specific heat data. Note that such field dependence of specific heat as shown in Figs. 4 and 5 is observed in 1D  $S = 1/2$  Heisenberg ferromagnets [10].

The lattice contribution to the specific heat in  $A_3\text{Cu}_3(\text{PO}_4)_4$  ( $A = \text{Ca}$ ,  $\text{Sr}$ , and  $\text{Pb}$ ) was estimated between 10 and 14 K using the expression  $C_l = \beta_1 T^3 + \beta_2 T^5$  ( $\beta_1 = 1.05(3) \times 10^{-3} \text{ J K}^{-4} \text{ mol}^{-1}$ ,  $\beta_2 = 5(2) \times 10^{-7} \text{ J K}^{-6} \text{ mol}^{-1}$  for  $A = \text{Ca}$ ,  $\beta_1 = 1.703(10) \times 10^{-3} \text{ J K}^{-4} \text{ mol}^{-1}$ ,  $\beta_2 = 1.1(6) \times 10^{-7} \text{ J K}^{-6} \text{ mol}^{-1}$  for  $A = \text{Sr}$ , and  $\beta_1 = 4.15(7) \times 10^{-3} \text{ J K}^{-4} \text{ mol}^{-1}$ ,  $\beta_2 = 1.3(4) \times 10^{-6} \text{ J K}^{-6} \text{ mol}^{-1}$  for  $A = \text{Pb}$ ) assuming magnetic contribution is negligible at these temperatures. The magnetic specific heat is not accurately zero, but it should be quite small because the influence from two Schottky-type anomalies is the smallest in this temperature range [3]. The  $\beta_1$  values give Debye temperatures,  $\Theta_D = (234Nk_B/\beta_1)^{1/3}$ , of 123, 104, and 78 K for  $A = \text{Ca}$ ,  $\text{Sr}$  and  $\text{Pb}$ , respectively. The magnetic entropy,  $S_m$ , associated with the long-range ordering is shown in Fig. 6.  $S_m$  saturates at about 5.11, 5.24, and 4.96  $\text{J K}^{-1} \text{ mol}^{-1}$  for  $A_3\text{Cu}_3(\text{PO}_4)_4$  with  $A = \text{Ca}$ ,  $\text{Sr}$ , and  $\text{Pb}$ , respectively. The entropy gained below the long-range ordering temperatures ( $T_N$  or  $T_C$ ) is 31%, 35%, and 42% of the saturated values for  $A_3\text{Cu}_3(\text{PO}_4)_4$  ( $A = \text{Ca}$ ,  $\text{Sr}$ , and  $\text{Pb}$ ), respectively. The entropy gained below  $T_N$  ( $T_C$ ) gives a barometer for the inter-chain interaction. For a good 1D system, less than about 10% of the entropy is gained below  $T_N$  ( $T_C$ ) and the remaining is gained slowly up to the temperature corresponding to  $J$ . Judging from above values, the inter-chain interactions are not negligible for the present systems compared with the intra-chain interaction ( $J_2$ ). This argument is consistent with the relatively large  $T_N/J_2$  values. The ground state of the linear trimer is a doublet with  $E(0) = -J_1$  and  $S_{\text{total}} = 1/2$  [11], that is, there is one Kramers doublet. The entropy change owing to the long-range ordering of the trimers is therefore expected to be  $R \ln 2 \approx 5.76 \text{ J K}^{-1} \text{ mol}^{-1}$ . The experimental  $S_m$  is smaller than the expected value probably due to the overestimation of the lattice contribution. Note that the reduced value

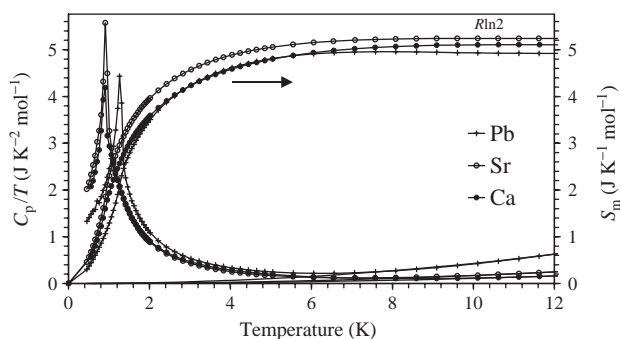


Fig. 6. The  $C_p/T$  vs.  $T$  and  $S_m$  vs.  $T$  curves at zero magnetic field for  $A_3\text{Cu}_3(\text{PO}_4)_4$  ( $A = \text{Ca}$ ,  $\text{Sr}$ , and  $\text{Pb}$ ).

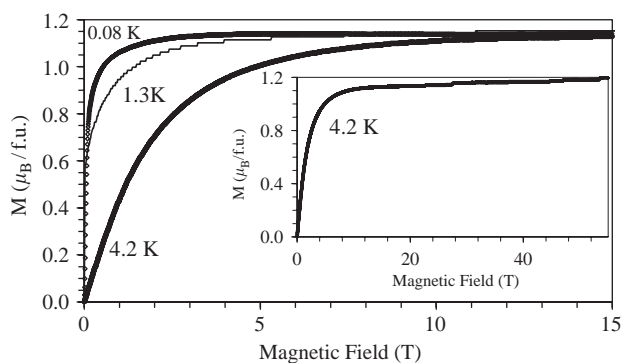


Fig. 7. The  $M$  vs.  $H$  curves at 0.08, 1.3, and 4.2 K for  $\text{Pb}_3\text{Cu}_3(\text{PO}_4)_4$  between 0 and 15 T. Inset gives the  $M$  vs.  $H$  curve at 4.2 K up to 55 T.

of  $S_m$  was also reported for the antiferromagnetic ordering of  $S = 1/2$  triangles in  $\text{La}_4\text{Cu}_3\text{MoO}_{12}$  [12].

The magnetization curves for  $A_3\text{Cu}_3(\text{PO}_4)_4$  ( $A = \text{Ca}$ ,  $\text{Sr}$ , and  $\text{Pb}$ ) saturate at about  $1.15$ – $1.20 \mu_B/\text{mol}$  (Fig. 7). This value is one-third of the expected saturation value,  $M_s$ , of  $3.45 \mu_B/\text{mol}$  for  $S = 1/2$  and  $g = 2.3$  [7]. The observed intermediate quantum state corresponds to  $S = 1/2$  per trimer. The  $1/3$  magnetization plateau persists up to 55 T at 1.3 and 4.2 K. The excitation energy from  $S_{\text{total}} = 1/2$  to  $S_{\text{total}} = 3/2$  is  $1.5J_1$  for the linear trimer model [11]. Applying  $J_1/k_B = 106$  K, estimated from the susceptibility data for  $\text{Pb}_3\text{Cu}_3(\text{PO}_4)_4$ , it is expected that the spin flip will be observed at  $H_{\text{sf}} \approx 103$  T.

No hysteresis was found on the  $M$  vs.  $H$  curves at 0.08 K for  $A_3\text{Cu}_3(\text{PO}_4)_4$  ( $A = \text{Sr}$  and  $\text{Pb}$ ), i.e., below the temperatures of long range ordering (Fig. 8). The  $M$  vs.  $H$  curves also pass through the origin. These facts give us evidence to believe that there is no net magnetic moment in the ground state of  $A_3\text{Cu}_3(\text{PO}_4)_4$  ( $A = \text{Sr}$  and  $\text{Pb}$ ), that is, they order antiferromagnetically. At about 0.03 T, the slope change of the  $M$  vs.  $H$  curves was detected in  $A_3\text{Cu}_3(\text{PO}_4)_4$  ( $A = \text{Sr}$  and  $\text{Pb}$ ) due to a spin flop transition in the antiferromagnetic state. The small value of the magnetic field for the spin flop transition reflects the small value of the inter-chain interaction.

The  $M$  vs.  $H$  curve of  $\text{Ca}_3\text{Cu}_3(\text{PO}_4)_4$  was different from those of  $A_3\text{Cu}_3(\text{PO}_4)_4$  ( $A = \text{Sr}$  and  $\text{Pb}$ ) and no spin-flop transition was observed in  $\text{Ca}_3\text{Cu}_3(\text{PO}_4)_4$ . Our data confirmed the different behavior of  $\text{Ca}_3\text{Cu}_3(\text{PO}_4)_4$  at very low temperatures in comparison with  $\text{Sr}_3\text{Cu}_3(\text{PO}_4)_4$  reported in the literature [4]. Taking into account the results of *ac* susceptibility measurements [4] and our  $M$  vs.  $H$  curves,  $\text{Ca}_3\text{Cu}_3(\text{PO}_4)_4$  orders ferromagnetically at  $T_C = 0.91$  K. The  $M$  vs.  $H$  curves indicates that  $\text{Ca}_3\text{Cu}_3(\text{PO}_4)_4$  behaves as a very soft ferromagnet because the  $M$  vs.  $H$  curves passed through the origin within the system resolution. The different behavior of  $\text{Ca}_3\text{Cu}_3(\text{PO}_4)_4$  and  $\text{Sr}_3\text{Cu}_3(\text{PO}_4)_4$  is interesting because they are isotopic with each other and have the same arrangement of the 1D trimeric chains.

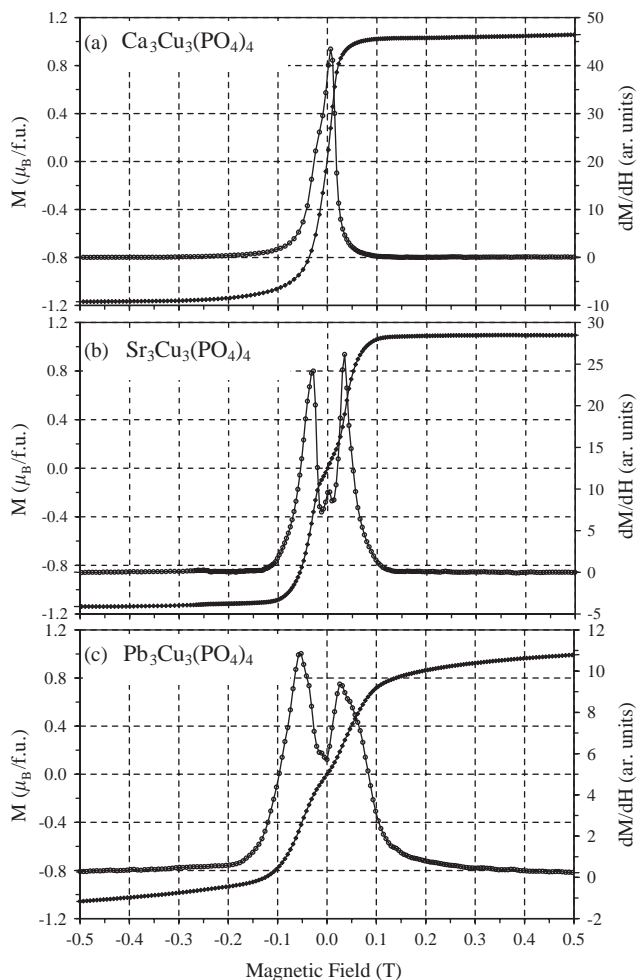


Fig. 8. The  $M$  vs.  $H$  (black diamonds) and  $dM/dH$  vs.  $H$  (circles) curves at 0.08 K for (a)  $\text{Ca}_3\text{Cu}_3(\text{PO}_4)_4$ , (b)  $\text{Sr}_3\text{Cu}_3(\text{PO}_4)_4$ , and (c)  $\text{Pb}_3\text{Cu}_3(\text{PO}_4)_4$  between  $-0.5$  and  $0.5$  T. These  $M$  vs.  $H$  curves were measured from 25 to about  $-3$  T.

In conclusion, we investigated magnetic properties of  $A_3\text{Cu}_3(\text{PO}_4)_4$  ( $A = \text{Ca}$ ,  $\text{Sr}$ , and  $\text{Pb}$ ). The paramagnetic moment decreases to  $S = 1/2$  per trimer below 45 K due to the antiferromagnetic intra-trimer interaction. The trimers exhibit ferromagnetic long-range ordering at  $T_C = 0.91$  K for  $A = \text{Ca}$  and antiferromagnetic long-range ordering at  $T_N = 0.91$  K for  $A = \text{Sr}$  and  $T_N = 1.26$  K for  $A = \text{Pb}$ . The intermediate  $1/3$ -magnetization plateau at 1.3 and 4.2 K persists up to 55 T. Below  $T_N$ , the clear spin flop transition is detected at low magnetic field in  $A_3\text{Cu}_3(\text{PO}_4)_4$  ( $A = \text{Sr}$  and  $\text{Pb}$ ). We observed strong field dependence of specific heat due to the finite intra-chain interaction ( $J_2$ ) in the 1D array of the trimers.

#### Acknowledgments

The authors express their thanks to the Ministry of Education, Culture, Sports, Science and Technology,

Japan, for Grants-in-Aid Nos. 13440111, 14204070, and 12CE2005 for COE Research on Elements Science, and for 21COE on the Kyoto Alliance for Chemistry.

## References

- [1] J.B. Anderson, E. Kostiner, F.A. Ruzsala, *J. Solid State Chem.* 39 (1981) 29.
- [2] A.A. Belik, A.P. Malakho, B.I. Lazoryak, S.S. Khasanov, *J. Solid State Chem.* 163 (2002) 121.
- [3] M. Drillon, M. Belaiche, P. Legoll, J. Aride, A. Boukhari, A. Moqine, *J. Magn. Magn. Mater.* 128 (1993) 83.
- [4] M. Drillon, E. Coronado, M. Belaiche, R.L. Carlin, *J. Appl. Phys.* 63 (1988) 3551.
- [5] A. Boukhari, A. Moqine, S. Flandrois, *Mater. Res. Bull.* 21 (1986) 395.
- [6] M. Matsuda, K. Kakurai, A.A. Belik, M. Azuma, M. Takano, M. Fujita, *Phys. Rev. B*, in press.
- [7] Y. Ajiro, T. Asano, K. Nakaya, M. Mekata, K. Ohoyama, Y. Yamaguchi, Y. Koike, Y. Morii, K. Kamishima, H. Aruga-Katori, T. Goto, *J. Phys. Soc. Jpn.* 70 (Suppl. A) (2001) 186.
- [8] H. Effenberger, *J. Solid State Chem.* 142 (1999) 6.
- [9] T. Nakanishi, S. Yamamoto, *Phys. Rev. B* 65 (2002) 214418.
- [10] K. Takeda, K. Konishi, K. Nedachi, K. Mukai, *Phys. Rev. Lett.* 74 (1995) 1673.
- [11] S.J. Gruber, C.M. Harris, E. Sinn, *J. Chem. Phys.* 49 (1968) 2183.
- [12] M. Azuma, T. Odaka, M. Takano, D.A. Vander Griend, K.R. Poppelmeier, Y. Narumi, K. Kindo, Y. Mizuno, S. Maekawa, *Phys. Rev. B* 62 (2000) R3588.